



Semnan University

Mechanics of Advanced Composite Structures

journal homepage: <http://MACS.journals.semnan.ac.ir>

Predicting Young's Modulus of Aggregated Carbon Nanotube Reinforced Polymer

R. Rafiee*, V. Firouzbakht

Composites Research Laboratory, Faculty of New Sciences and Technologies, University of Tehran, Tehran, 1439955941, Iran

PAPER INFO

Paper history:

Received 18 April 2014

Received in revised form 15 June 2014

Accepted 24 June 2014

Keywords:

Carbon nanotube
Multi-scale modeling
Irregular tessellation
Stochastic modeling

ABSTRACT

Prediction of mechanical properties of carbon nanotube-based composite is one of the important issues which should be addressed reasonably. A proper modeling approach is a multi-scale technique starting from nano scale and lasting to macro scale passing in-between scales of micro and meso. The main goal of this research is to develop a multi-scale modeling approach to extract mechanical properties of CNT based nanocomposites emphasizing on meso-scale parameters. Agglomeration and non-straight shapes of CNTs have to be captured in this specific scale. The representative volume element (RVE) for meso-scale is identified considering local concentration of CNTs as the main source of inhomogeneity in the investigated material region. Irregular tessellation technique on the basis of Voronoi method and Bayes algorithm is employed to partition the RVE at meso scale into constitutive polygons containing one single aggregate. A MATLAB code is written to perform this stage on the basis of random pattern. Mechanical properties of the tasseled regions are extracted by a combination of micromechanics rule addressing local position and aggregates in the material region. A bounding technique accounting for non-straight shape of CNT is utilized to consider the any arbitrary shape of wavy CNT. Investigated material region at macro scale is divided into constitutive blocks assigning random volume fractions of CNT to each block implying non-uniformed dispersion of CNT. The results demonstrate the importance of considering the position of local aggregates in modeling procedure. The obtained results of modeling are compared with experimentally measured mechanical properties.

© 2014 Published by Semnan University Press. All rights reserved.

1. Introduction

The outstanding, exceptional, mechanical, electrical and thermal properties of Carbon Nanotubes (CNTs) [1-4] have stimulated researchers to exploit them as a new generation of reinforcing agents for polymers. Incorporating small amounts of CNTs into polymer and experimentally observed significant growth in the mechanical properties of polymer [5-7] has established a new era in the field of advanced materials. Therefore, predicting mechanical properties of the CNT/polymer composites on the basis of constituent's mechanical properties not only plays

an important role in their development process, but also has received lots of attractions among researchers in the last decade. Developed micromechanics rules cannot be directly used for the case of CNT/polymer [8-18]. The basic assumptions of the micromechanics rules are not valid for CNT/polymer. Basically, micromechanics rules treat the reinforcing phase as a continuum medium which is not pertinent to the lattice structure of CNT. They also take into account perfect bonding between reinforcing agent and surrounding polymer; while CNT interacts with surrounding polymer through non-bonded van der Waals (vdW) interactions.

* Corresponding author. Tel.: +98-21-61118506; Fax: +98-2188617081

E-mail address: Roham.Rafiee@ut.ac.ir

Moreover, formation of locally concentrated aggregates due to CNT agglomeration and also the non-straight shapes of CNTs arisen from their high aspect ratios cannot be captured by micromechanics rules. These phenomena will diminish the efficiency of CNTs in reinforcement and should be captured reasonably.

Different researchers have tried to modify available micromechanics rule for CNT-based composites [19-30]. It can be seen from literature that all performed studies in the field of modifying micromechanics rule for the purpose of CNT-based composites suffer from different shortcomings. Almost all conducted studies are performed on the basis of curve fitting to the observed experimental results. Due to the generic philosophy of their development, the applications of these formulations are limited to the special cases wherein exactly same conditions are governed to the materials. Therefore, the applicability of these formulations to the new sets of experimental data is under question. Furthermore, the predicted results by developed formulations are compatible with experimental data either in the lower ranges of CNT contents or in the higher values. Namely, they are not consistent with experimental data in both low and high CNT contents with the same level of accuracy. More importantly, developed formulations do not cover all intrinsic deficiencies associated with CNT in reinforcing polymer and just some of them have been captured. The essential issues weakening the capability of CNT in reinforcing polymers can be classified into five main groups of non-uniformed dispersion, non-aligned, agglomerated, non-straight shapes of CNTs and non-bonded interactions between CNT and surrounding polymers in the interphase region.

The main goal of this research is to establish a perfect virtual laboratory for calculating the Young's modulus of CNT-based composites taking into account all inconsistencies arisen from processing of CNT-based nanocomposites. So, appropriate multi-scale modeling covered all scales of Nano, Micro, Meso and Macro is employed to predict Young's modulus of CNT reinforced polymer (CNTRP). The employed multi-scale modeling is able to simulate all effective parameters at corresponding scales. Finally, the obtained results are compared with nearby theoretical multi-scale approaches ensuring its abilities.

2. Problem Statement

Due to the wide range of the scales associated with CNTRP, a multi-scale modeling is required to predict mechanical properties of investigated mate-

rial. All involved length scales, starting from atomic scale and lasting to bulk material level are scanned in this approach. A proper bridging between physical governing conditions at atomic level and the material behavior at the macro level depends on the development of a model considering all nano, micro, meso and macro scales. It should be noted that proper RVEs¹ must be defined at each scale and all the phenomena related to them should be considered at the proper scale of occurrence.

Thanks to the complexity of this approach, few researchers have applied it in the field of nanocomposites [12, 31-35]. Spanos and Kotsos [34] have developed a full-range multi-scale modeling while just CNT volume fraction has been treated as single random parameter. Shokrieh and Rafiee [35] developed a full-stochastic and full range multi-scale modeling, called N3M, treating all CNT length, orientation, volume fraction, non-straight shape and agglomeration as random parameters.

N3M multi-scale modeling is selected in this research as the foundation of multi-scale modeling procedure. Some improvements will be provided to the previously developed N3M modeling [35] at the specific scales of meso and macro in order to simulate bundled CNTs more accurately. In contrast with [35] wherein regular tessellation technique is used at meso scale, irregular tessellation technique is developed in this research in order to take into account the local position of each aggregate. In other words, while developed modeling in [35] simply neglects the local position of each aggregate in meso scale RVE, this issue is taken into account in this research.

3. Multi-Scale Modeling

Due to the important issues occurring at meso and macro scales, these two scales are mainly focused in this research. Local agglomerations, non-straight shapes and random orientations of CNTs have to be taken into account at meso scale [35]. While the effective scales of other issues like CNT length and interphase between CNT and surrounding polymer are nano and/or micro scales, uniformed or non-uniformed dispersion of aggregates is treated at macro scale [35].

3.1. Top-Down Scanning

The RVE at macro scale is the bulk material region which is partitioned into constitutive blocks at meso scale. The bulk material is partitioned into

¹ Representative Volume Element

small rectangle elements using regular tessellation method.

A random CNT volume fraction is allocated to each block which is consistent with the global CNT volume fraction. Thus, heterogeneous environment of the material due to non-uniformed distribution of CNTs in the resin is captured. After partitioning of RVE at macro scale into its constitutive blocks at meso scale using regular tessellation method, the mechanical properties of each block at meso scale should be derived.

The embedded CNTs in the meso-scale RVE can be either concentrated in local regions forming aggregates or dispersed in some other areas representing fully dispersed CNTs. Irregular tessellation on the basis of Voronoi approach [36] is used to partition the RVE at meso-scale into constitutive polygons. In this method, each constitutive polygon consists of a special point called generator or seed. All the other points located inside the polygon and in neighboring areas of a seed are at the lowest distance to the seed rather than the other points. All points placed on the edges of each polygon are at the same distance to the two neighbor seeds. Therefore, if it is assumed that each specific seed represents only one single aggregate, the locations of aggregate play an important role in determining mechanical properties of the RVE at meso-scale. Then, each obtained polygon is converted into a spherical element assuming its center as a seed. The procedures of regular tessellation at macro scale and irregular tessellation technique on the basis of Voronoi approach [36] are presented in Figure 1.

Following the explained procedure of irregular tessellation technique, each constitutive block at meso-scale will be converted to the assemblage of spheres with different radii. Radius and surface area of each sphere can vary from very low to high values depending on the parent polygon. the neighboring areas have the minimum distance to it rather than

other center points of other spheres. Consequently, the RVE at meso scale is tessellated into spherical particles with various diameters surrounded by spherical surfaces of matrix. There is no interference between spheres and the adjacent elements are tangent together.

An example of such clustering is schematically presented in Figure 2.

An exact closed form solution is developed to obtain mechanical properties of such spherical element assemblage in this tessellated structure. This model is also called Composite Sphere Assemblage (CSA) [38, 39].

In order to create the constitutive polygons in the rectangular element at meso-scale based on Voronoi algorithm, the coordinates of seeds have to be specified in the x-y plane. The number of seeds depends on the number of polygon elements. Bayes algorithm is used for defining the locations of seeds [40]. Based on Bayes algorithm, normal distribution is considered for the coordinates of the seed points.

The coordinates of each seed are selected as the mean value for the normal distributions of other points located on the distribution curves centered on the seeds. In other words, all of the points located on the plane have several special numbers, each of which is related to a specified seed.

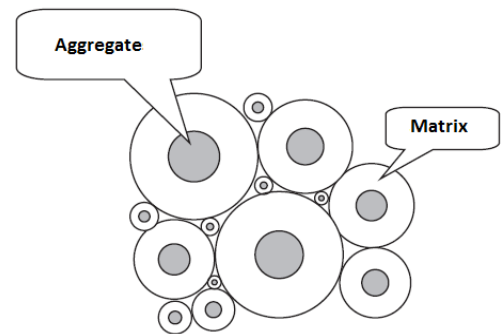


Figure 2. Quasi-Spherical Tessellation [37]

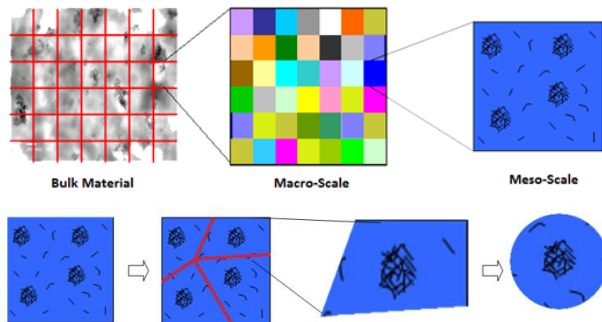


Figure 1. RVEs at Macro and Meso Scales

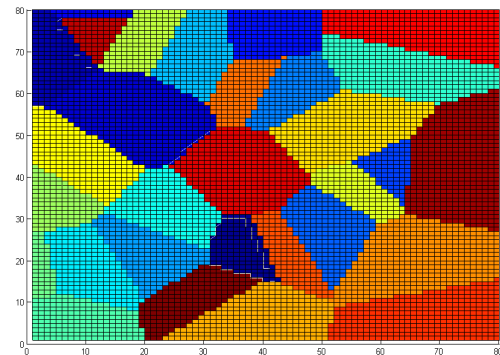


Figure 3. Voronoi cells created by Bayes Algorithm

The bigger value assigned to a point implies the closer point to the corresponding seed. For each point, the biggest value is taken into account neglecting other values. Therefore, every point will be located on a single distribution curve. The distance between all points located on a curve and the peak of the curve (mean value representing seed) present the smallest value in comparison with other seeds.

These curves will produce conic surfaces on 3D space which the points located in the foothills are at the minimum distance from the seeds (tip of the cones). Voronoi polygons are formed by projecting the 3D cones on the bottom plane as illustrated in the Figure 3.

3.2. Bottom-Up Modeling

Bottom-up modeling in the form of hierarchical multi-scale modeling is employed to obtain Young's modulus of the CNTRP. The modeling starts from the scale of nano. Equivalent fiber phenomenon developed by Shokrieh and Rafiee [38-40] is used. The equivalent fiber consists of the CNT and the inter-phase region between CNT and polymer. The lattice and hollow structure of the CNT interacting with surrounding polymer through the non-bonded van der Waals interaction is replaced with a virtually solid fiber representing equivalent fiber. Since the CNTs have different lengths, the properties of the equivalent fiber vary with the CNT length. According to the results of a parametric study on the effects of CNT length on the mechanical properties of equivalent fiber, the mechanical properties of the equivalent fiber associated with the mean length of 500 nm are used. As it can be seen from the properties reflected in table 1, the equivalent fiber exhibits transversely-isotropic behavior.

According to the CNT volume fraction dedicated to each rectangular constitutive block at macro-scale, the portion of each Voronoi cell which is created inside of them at meso-scale can be also defined randomly. Each polygon can be considered as a spherical element after applying CSA method, wherein the inner circle represents aggregated CNTs surrounded by fully dispersed CNTRP as the outer circle. Thus, properties of these two distinct phases in the spherical elements should be obtained [41, 42]. Since the size of each spherical element is

different from the other ones, a random logic has to be applied to determine the local CNT volume fraction allocated to each phase. For this purpose, random coefficients representing concentration of CNTs in both inner and outer circles are considered. Following improved Mori-Tanaka model, the CNT volume fraction assigned to each spherical element is divided into two phases [43]:

$$V_{CNT} = V_{CNT}^{inclusion} + V_{CNT}^m \quad (1)$$

The random coefficients representing agglomeration phenomena are defined as follows [43]:

$$\mu = \frac{V_{inclusion}}{V}, \quad \kappa = \frac{V_{CNT}^{inclusion}}{V_{CNT}} \quad (2)$$

where $V_{inclusion}$ is the volume of spherical particles, and V is the total volume of the spheres. μ represents the ratio of total aggregates particles to the total volume of RVE and κ is the ratio of CNT volume fraction inside the aggregates to the total CNT volume fraction in spherical elements. The local volume fraction of CNTs allocated to each phase is obtained from the following relations [43]:

$$\frac{V_{CNT}^{inclusion}}{V_{inclusion}} = \frac{f_{CNT} \kappa}{\mu}, \quad \frac{V_{CNT}^m}{V - V_{inclusion}} = \frac{f_{CNT} (1 - \kappa)}{1 - \mu} \quad (3)$$

where f_{CNT} is obtained using:

$$f_{CNT} = \frac{V_{CNT}}{V} \quad (4)$$

The mechanical properties of each phase can now be extracted by using micromechanics rule developed by Hashin [41] and Christensen [42]:

$$K_{in} = K_m + \frac{\frac{f_{CNT} \kappa}{\mu} (K_r - K_m)}{\left(1 - \frac{f_{CNT} \kappa}{\mu}\right) (K_r - K_m) + 1 + \frac{\mu}{\left(K_m + \frac{4}{3} G_m\right)}} \quad (5)$$

$$K_{out} = K_m + \frac{\frac{f_{CNT} (1 - \kappa)}{1 - \mu} (K_r - K_m)}{\left(1 - \frac{f_{CNT} (1 - \kappa)}{1 - \mu}\right) (K_r - K_m) + 1 + \frac{1 - \mu}{\left(K_m + \frac{4}{3} G_m\right)}} \quad (6)$$

Table 1. Mechanical Properties of the Equivalent Fiber [38-40]

Longitudinal Young's Modulus [GPa]	Transverse Young's Modulus [GPa]	Shear Modulus [GPa]	Poisson's Ratio
348	11.27	5.13	0.284

$$G_{in} = G_m + \frac{\frac{f_{CNT} \kappa}{\mu}}{\frac{1}{G_r - G_m} + \frac{6(K_m + 2G_m)(1 - \frac{f_{CNT} \kappa}{\mu})}{5G_m(3K_m + 4G_m)}} \quad (7)$$

$$G_{out} = G_m + \frac{\frac{f_{CNT}(1 - \kappa)}{1 - \mu}}{\frac{1}{G_r - G_m} + \frac{6(K_m + 2G_m)(1 - \frac{f_{CNT}(1 - \kappa)}{1 - \mu})}{5G_m(3K_m + 4G_m)}} \quad (8)$$

where superscripts of “in” and “out” denote inner sphere or aggregate and outer sphere reflecting fully dispersed CNT in matrix, respectively. The superscripts of “m” and “r” stand for matrix and equivalent fiber. Finally, mechanical properties of each two-phase spherical inclusion representing polygon elements are obtained as below:

$$K = K_{out} + \frac{\mu(K_{in} - K_{out})}{1 + \frac{(1 - \mu)(K_{in} - K_{out})}{\left(K_{out} + \frac{4}{3}G_{out}\right)}} \quad (9)$$

$$G = G_{out} + \frac{\mu}{\frac{1}{G_{in} - G_{out}} + \frac{6(K_{out} + 2G_{out})(1 - \mu)}{5G_{out}(3K_{out} + 4G_{out})}} \quad (10)$$

$$E = \frac{9KG}{3K + G} \quad (11)$$

The mechanical properties of the reinforcing agent (Kr and Gr) are calculated using equivalent fiber properties inserted in table 1.

To consider the effect of CNT waviness at the meso scale, a phenomenological technique is used [44]. Thanks to the transversely isotropic behavior of the equivalent fiber, the modulus of a unit-cell containing an embedded non-straight CNT in polymer can be bounded between two extreme values dictated by longitudinal and transverse moduli of the unit-cell. As a subsequent, the effective modulus of a non-straight fiber is placed between the bounding values dictated by longitudinal and transverse effective moduli of a straight equivalent fiber. Consequently, the random selection of the modulus between bounding values obtained for the straight equivalent fiber will capture any arbitrary non-straight shapes of CNTs. Following this procedure, the associated properties with the straight equivalent fiber presented in equations (5) to (8) are replaced with randomly selected values between

bounding values. After obtaining the mechanical properties of polygons and subsequently the building blocks at meso scale, the mechanical properties of the bulk material at macro scale is obtained using averaging method. The process is implemented in a written computer code on the MATLAB platform.

Since the developed algorithm for the creation of a polygon follows a fully stochastic process, none of the blocks have the same tessellation pattern. Moreover, all dispersion, agglomeration and waviness of CNTs as the most important parameters at macro and meso scales are random parameters. A convergence study is performed to extract three parameters of number of constitutive blocks at macro scale, number of Voronoi polygons at meso scale and number of realizations. A convergence criterion is defined as 0.1% for the coefficient of variation for the Young’s modulus of the whole material region at macro scale. It is observed that 300 realizations of stochastic method on a 30×30 region consisting of 7 seeds in each block fulfill the requirements of the convergence criterion.

Table 2. Comparison between predicted results with published experimental data

Researcher(s)	Constituents Properties		Young’s Modulus [GPa]		
	Matrix Modulus [GPa]	CNT Volume Fraction (%)	Measured By Experiment	Modeling	Error (%)
Villoria & Miravete [11]	2.875	0.12	2.909	2.917	-0.2
	2.587	0.47	2.659	2.651	0.3
Ogasawara et al.[45]	2.84	2.3	3.07	2.96	3.5
	2.84	5.4	3.28	3.19	2.7
	2.84	10.3	3.90	3.75	3.8
Kanagaraj et al. [46]	1.095	0.11	1.169	1.155	1.1
	1.095	0.22	1.228	1.232	-0.3
	1.095	0.33	1.287	1.286	0.07
	1.095	0.44	1.338	1.323	1.09
Xiao et al. [47]	0.235	1	0.261	0.252	3.4
	0.235	3	0.284	0.264	0.7
	0.235	5	0.386	0.359	6.9
	0.235	10	0.444	0.418	5.8

4. Results and Discussion

In order to check the accuracy of the developed modeling procedure, obtained results are compared with available experimental observations in literature. It should be pointed out that all CNT volume fractions, orientations, agglomerations and non-straight shapes have been treated as random variables in accordance with explained procedure of modeling in section 3. As shown in Table 2, there is a very good agreement between obtained results and experimental observations.

As it can be seen from a comparison presented in Table 2, in very rare cases the developed theoretical modeling overestimates Young's modulus with very low error percentage.

A detailed investigation is carried out to understand the degree to which inconsistencies affect the properties. It is revealed that the most important parameter is the non-straight CNT shape and after that local concentration of CNTs into aggregated plays an important role in decreasing mechanical properties of CNTRP from ideal cases.

Another comparison is carried between developed modeling with N3M modeling [35] and the results are presented in Table 3. A very good agreement between obtained results using these

two different techniques accompanied by considerable reduction in the runtime of the modeling procedure implies the efficiency of the developed modeling. It should be pointed out that due to the employed technique of irregular tessellation at meso scale, the current modeling technique is able to take into account the position of aggregates, as it is not possible by employing N3M modeling [35].

5. Conclusion

In this study, a multi-scale approach is used for modeling CNT-based composites focusing on the phenomena associated with the meso and macro scales. Regular tessellation technique is used to partition material region at macro scale to the constitutive blocks with random volume fraction addressing non-uniformed dispersion of CNTs.

A new method is developed at meso scale for irregular tessellation of the constitutive block using Bayes classification algorithm combined with Voronoi method. Each constitutive block is tessellated to the heterogeneous polygons on the basis of irregular pattern capturing aggregated CNTs. Each of the polygons has a single agglomeration and so their locations are taken into account. Each polygon is converted into the two-phase sphere containing an aggregated CNTs surrounded by dispersed CNT in matrix using Composite Cylinder Assemblage model. The proposed formulation by Hashin [41] and Christensen [42] are modified accounting for agglomeration and properties of each polygon obtained accordingly. Equivalent fiber theory [38-40] has been used to consider non-bonded interphase region between CNT and surrounding polymer at micro scale. Thanks to the equivalent fiber theory, the non-straight shapes of the CNTs are simulated using phenomenological bounding technique. Full stochastic multi-scale modeling is implemented treating all agglomeration, non-uniformed dispersion and wavy pattern of CNTs as random parameters. Finally, comparing the obtained results with previously introduced N3M method [35] and also previously published experimental data, very good consistency is observed with better clarification of random parameters in Meso scale and more time-efficient by lower runtime.

References

- [1] Dai H. Carbon nanotubes: opportunities and challenges. *Surf Sci* 2002; 500(1-3): 218-41
- [2] Kang, Heung YY, Kim JH, Lee JW, Gollapudi R, Subramaniam S, et al. Introduction to carbon nanotube and nanofiber smart materials, *Compos. Part B-Engineering* 2006; 37(6): 382-94

Table 3. Comparison of the obtained results with N3M results [35]

CNT Volume fraction (%)	Matrix Modulus [GPa]	Young's modulus [GPa]		
		N3M (error (%))	Current model (error (%))	Experimental observation
0.1	0.85	0.847 (3.2)	0.857 (2.06)	0.875
0.5	0.85	1.152 (4)	1.168 (2.67)	1.2
1.0	0.85	1.32 (5.7)	1.34 (4.29)	1.4
0.882	2.026	2.514 (5.1)	2.564 (3.25)	2.65
3.306	2.026	3.223 (6.3)	3.34 (2.91)	3.44
2.28	4	5.26 (6)	5.41 (3.39)	5.6
4.58	4	5.77 (6.8)	5.91 (4.68)	6.2
0.187	0.855	1.013 (0.6)	1.012 (0.78)	1.02
0.37	0.855	1.09 (0.9)	1.092 (0.73)	1.1
0.563	0.855	1.163 (1.14)	1.168 (1.02)	1.18

- [3] Salvétat-Delmotte JP, Rubio A. Mechanical properties of carbon nanotubes: a fiber digest for beginners. *Carbon* 2002; 40(10): 1729-734
- [4] Lau KT, Gu C, Hui D. A critical review on nanotube and nanotube/nanoclay related polymer composite materials, *Compos Part B-Engineering* 2006; 37(6): 425-36
- [5] Qian D, Dickey E, Andrews R, Rantell T. Load transfer and deformation mechanisms in carbon nanotube-polystyrene composites, *Appl Phys Lett* 2000; 76(20): 2868-870
- [6] Schadler L, Giannaris SC, Ajayan PM. Load transfer in carbon nanotube epoxy composites, *Appl Phys Lett* 2000; 73(26): 3842-844
- [7] Zhu J, Peng H, Rodriguez-Macias F, Margrave J, Khabashesku V, Imam A, Lozano K, Barrera E. Reinforcing epoxy polymer composites through covalent integration of functionalized nanotubes, *Adv Funct Mater* 2004; 14(7): 643-48
- [8] Odegard GM, Gates TS, Wise KE, Park C, Siochi EJ. Constitutive modeling of nanotube-reinforced polymer composites, *Compos Sci Technol* 2003; 63(11): 1671-687
- [9] Ashrafi B, Hubert P. Modeling the elastic properties of carbon nanotube array/polymer composites, *Compos Sci Technology* 2006; 66(3-4): 387-96
- [10] Han Y, Elliott J. Molecular dynamics simulations of the elastic properties of polymer/carbon nanotube composites, *Compos Mater Sci* 2007; 39 :315-23.
- [11] Villoria RG, Miravete A. Mechanical model to evaluate the effect of the dispersion in *nano-composites*, *Acta Mater* 2007; 55(9) 3025-031
- [12] Tserpes KI, Panikos P, Labeas G, Panterlakis SpG, Multi-scale modeling of tensile behavior of carbon nanotube-reinforced composites, *Theor Appl Fract mech* 2008; 49(1): 51-60
- [13] Frankland SJV, Harik VM, Odegard GM, Brenner DW, Gates TS. The stress-strain behavior of polymer-nanotube composites from molecular dynamics simulation, *Compos Sci Technol* 2003; 63(11): 1655-661
- [14] Mokashi VV, Qian D, Liu Y. A study on the tensile response and fracture in carbon nanotube-based composites using molecular mechanics, *Compos Sci Technol* 2007; 67(3-4): 530-40
- [15] Shokrieh MM, Rafiee R. On the tensile behavior of an embedded carbon nanotube in polymer matrix with non-bonded interphase region, *Compos Struct* 2010; 92(3): 647-52
- [16] Selmi A, Friebel C, Doghri I, Hassis H. Prediction of the elastic properties of single walled carbon nanotube reinforced polymers: A comparative study of several micromechanical models, *Compos Sci Technol* 2007; 67(10): 2071-084
- [17] Seidel GD, Lagoudas DC. Micromechanical analysis of the effective elastic properties of carbon nanotube reinforced composites, *Mech Mater* 2006; 38(8-10): 884-907
- [18] Liu Y, Nishimura N, Otani Y. Large-scale modeling of carbon-nanotube composites by a fast multipole boundary element method, *Comput Mater Sci* 2005; 34(2): 173-87
- [19] Thostenson ET, Ren Z, Chou TW. Advances in the science and technology of carbon nanotubes and their composites: a review, *Compos Sci Technol* 2001; 61(13): 1899-912
- [20] Anumandla V, Gibson RF. A comprehensive closed form micromechanics model for estimating the elastic modulus of nanotube-reinforced composites, *Compos Part A* 2006; 37(12):2178-185
- [21] Yeh MK, Tai NH, Liu JH. Mechanical properties of phenolic-Based nanocomposites reinforced by multi-walled carbon nanotubes and carbon fibers, *Compos Part A* 2008; 39(4):677-84
- [22] Shao LH, Luo RY, Bai SL, Wang J. Prediction of effective moduli of carbon nanotube-reinforced composites with waviness and debonding, *Compos Struct* 2009; 87(3): 274-281
- [23] Montazeri A, Javadpour J, Khavandi A, Tchar-khtchi A, Mohajeri A. Mechanical properties of multi-walled carbon nanotube/epoxy composites, *Mater Des* 2010; 31: 4202-208
- [24] Shady E, Gowayed Y. Effect of nanotube geometry on the elastic properties of nanocomposites, *Compos Sci Technol* 2010; 70(10): 1476-481
- [25] Omidi M, Rokni DTH, S.Milani A, Seethaler RJ, Arasteh R. Prediction of the mechanical characteristics of multi-walled carbon nanotube/epoxy composites using a new form of the rule of mixtures, *Carbon* 2010; 48(11): 3218-228
- [26] Fisher FT, Bradshaw RD, Brinson LC. Fiber waviness in nanotube-reinforced polymer composites—I: modulus predictions using effective nanotube properties, *Compos Sci Technol* 2003; 63(11): 1689-1703
- [27] Bradshaw RD, Fisher FT, Brinson LC. Fiber waviness in nanotube-reinforced polymer composites: II. Modeling via Numerical approximation of the dilute strain concentration tensor. *Compos Sci Technol* 2003; 63(11): 1689-1703
- [28] Ayatollahi MR, et al. Effect of multi-walled carbon nanotube aspect ratio on mechanical and electrical properties of epoxy-based nanocomposites. *Polym Test* 2011; 30(5): 548-56.

- [29] Martone A, Faiella G, Antonucci V, Giordano M, Zarrelli M. The effect of the aspect ratio of carbon nanotubes on their effective reinforcement modulus in an epoxy matrix, *Compos Sci Technol* 2011; 71(8): 1117–1123
- [30] Srivastava VK, Singh S. A Micro-Mechanical model for elastic modulus of multi-walled Carbon-Nanotube/Epoxy resin composites, *Int J of Composite Materials* 2012; 2(2): 1-6.
- [31] Li C, Chou TW. Multiscale modeling of carbon nanotube reinforced polymer composites, *Nanosci Nanotechnol* 2003; 3(5): 423-30.
- [32] Tsai JL, Tzeng SH, Chiu YT, Characterizing elastic properties of carbon nanotubes/polyimide nanocomposites using multi-scale simulation, *Compos. Part B-Engineering* 2010; 41: 106-115
- [33] Luo D, Wang WX, Takao Y. Effects of the distribution and geometry of carbon nanotubes on the macroscopic stiffness and microscopic stresses of nanocomposites, *Compos Sci Technol* 2007; 67(14): 2947–2958
- [34] Spanos PD, Kotsos A. A multiscale monte carlo finite element method for determining mechanical properties of polymer nanocomposites, *Probabilis Eng Mech* 2007; 23(4): 456-70
- [35] Shokrieh MM, Rafiee R. Development of a full range multi-scale model to obtain elastic properties of CNT/polymer composites. *Iran Polym J* 2012; 21: 397–402
- [36] Okabe A, Boots B, Kokichi Sugihara K, Chiu SN. *Spatial Tessellations – Concepts and Applications of Voronoi Diagrams*. 2nd edition. John Wiley; 2000
- [37] Mishnaevsky Jr. *Computational esomechanics of composites*. John Wiley; 2007
- [38] Shokrieh MM, Rafiee R. Investigation of nanotube length effect on the reinforcement efficiency in carbon nanotube based composites, *Compos Struct* 2010; 92 (10): 2415-420
- [39] Shokrieh MM, Rafiee R. Prediction of mechanical properties of an embedded carbon nanotube in polymer matrix based on developing equivalent long fiber, *Mech Res Commun* 2010; 37(2):235-240
- [40] Shokrieh MM, Rafiee R. On the tensile behavior of an embedded carbon nanotube in polymer matrix with non-bonded interphase region, *Compos Struct* 2010; 92(3): 647-652
- [41] Hashin,Z. The elastic moduli of heterogeneous materials, *Appl Mech* 1962; 29: 143–150
- [42] Christensen, RM. *Mechanics of Composite Materials*. New York: Wiley-Interscience; 1979
- [43] Shi DL, Feng XQ, Huang YY, Hwang KC, Gao H. The effect of nanotube waviness and agglomeration on the elastic property of carbon nanotube-reinforced composite, *Eng Mater Technol* 2004; 126: 250-57
- [44] Rafiee R. Influence of carbon nanotube waviness on the stiffness reduction of CNT/polymer composites, *Compos Struct* 2013; 97: 304-09.
- [45] Ogasawara T, Ishida Y, Ishikawa T, Yokota R. Characterization of multi-walled carbon nanotube/phenylethynyl terminated polyimide composites. *Compos Part A* 2004; 35(1): 67–74.
- [46] Kanagaraj S, Varanda FR, Zhiltsova TV, Oliveira MSA, Simoes JAO. Mechanical properties of high density polyethylene/carbon nanotube composites. *Compos Sci Technol* 2007; 67(15-16): 3071-3077
- [47] Xiao SP, Zhang LC, Zarudi I. Mechanical and rheological properties of carbon nanotube-reinforced polyethylene composites. *Compos Sci Technol* 2007; 67(2): 177-82.